Determination of phase diagrams for the hard-core attractive Yukawa system

M. H. J. Hagen and D. Frenkel

FOM Institute for Atomic and Molecular Physics, Kruislaan 407, 1098 SJ Amsterdam, The Netherlands

The phase diagram of a system consisting of hard particles with an attractive Yukawa interaction is computed by Monte Carlo simulation. From the results of these simulations we can estimate that the liquid–vapor coexistence curve disappears when the range of the attractive part of the Yukawa potential is less than approximately one-sixth of the hard-core diameter. The results of the simulations are compared with predictions based on first order perturbation theory.

I. INTRODUCTION

The range of the attractive part of the intermolecular potential determines whether or not a given substance can have a stable liquid phase. This observation was made in the context of colloid science when Gast, Hall, and Russel reported a theoretical study of the phase diagram of colloid–polymer mixtures.[1] In the model used by these authors,[2,3] the presence of free polymer induces an attractive interaction between the (hard-core) colloids. The range of this interaction is determined by the radius of gyration of the polymers. In Ref. 1, the phase diagram was estimated using perturbation theory and it was found that when R_g, the radius of gyration of the polymer, is sufficiently large ($R_g/\sigma \geq 0.3$), the colloidal system can exist in a solidlike, liquidlike, and vaporlike state. However, for smaller polymers (short ranged attraction), the liquid phase disappears and only the solid and the "fluid" phases remain. Subsequent theoretical work by Lekkerkerker *et al.*,[4] experiments by Pusey[5] and Leal Calderon[6] and computer simulations by Meijer and Frenkel[7] indicate that the colloidal liquid–vapor transition does indeed disappear for sufficiently short-ranged attractive interactions between the colloidal particles. Thus far, there is limited evidence that the liquid–vapor transition can be made to disappear in simple atomic or molecular fluids. The reason is that for most molecular substances, the ratio of the ranges of the attractive and repulsive interactions are such that a liquid–vapor transition is to be expected. In particular, all particles interacting through an effective pair potential that can be approximated by the famous Lennard-Jones 12-6 potential, should have a liquid–vapor transition (see Ref. 8). Only for C_{60}, a molecule with an anomalously narrow attractive well, is there numerical evidence[9] that the liquid–vapor transition should be absent. Apart from that, there has been hardly any systematic attempt to study, by computer simulation, the relation between the range of the attraction part of the intermolecular potential and the stability of the liquid phase, for simple one-component model systems. In the present paper, we report a numerical study of a simple model fluid with a variable-range attractive interaction, namely a hard-sphere fluid with an attractive Yukawa interaction

$$u(r) = \begin{cases} \infty & (r < \sigma) \\ -\epsilon \dfrac{\exp[\kappa\sigma(1 - r/\sigma)]}{r/\sigma} & (r \geq \sigma) \end{cases} \quad (1)$$

where σ is the diameter of the hard core, ϵ is the well depth, and κ^{-1} is a measure for the range of the attractive part of the potential. Note that the well depth ϵ defines our unit of temperature. In what follows we shall use reduced units such that $\epsilon = 1$ and $\sigma = 1$. Figure 1 shows the shape of this interaction potential for the values of κ studied in this paper. We have chosen to study the hard-core attractive Yukawa model because, while it is a simple pair potential, it is known to provide a reasonable approximation of the polymer-induced interaction between a pair of hard colloidal particles (see, e.g., Refs. 2 and 7). Hence, the results of the present simulations should provide a reasonable estimate of the phase behavior of polymer colloid mixtures.

In order to map out the phase diagram of the hard-core Yukawa model, we combine Gibbs-ensemble Monte Carlo simulation to determine the liquid–vapor coexistence curve[10,12] with the Gibbs–Duhem integration method of Kofke.[14,15] The latter method is well suited to compute the solid–liquid coexistence line, starting from the (known) coexistence properties of the hard-sphere model. The latter model corresponds to the infinite temperature limit of the attractive Yukawa system.

In the following section, we briefly describe the simulation methods used. We then present the phase diagram of the hard-core Yukawa system, as obtained from our Monte Carlo simulations. Finally, we compare our simulation results with the predictions of first-order perturbation theory.

II. SIMULATIONS

In order to map out the phase diagram of the hard-core attractive Yukawa model, we have used, as much as possible, methods that allow us to limit our simulations to points located on the coexistence curves. For liquid–vapor coexistence, this can be achieved by employing the Gibbs-ensemble method of Panagiotopoulos.[10,12] In this method, two simulations are carried out in parallel; one of the liquid phase and one of the vapor. The two systems are held at the same temperature and are allowed to exchange volume and mass, but the total volume and total number of particles of the two systems is fixed. This ensures that, at equilibrium, the pressure and chemical potential of the two systems are the same. As a consequence, the conditions for phase coexistence are automatically satisfied. The Gibbs ensemble technique cannot be used to study solid–fluid coexistence, because ex-
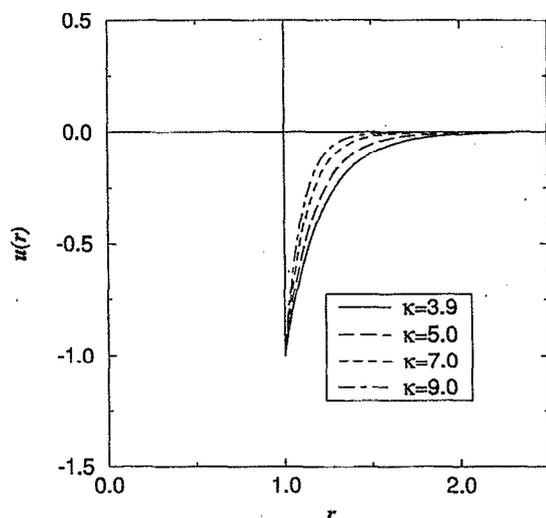
FIG. 1. Interaction potential.

TABLE I. Coexisting vapor–liquid densities for different reciprocal temperatures β for two values of κ as obtained from Gibbs-ensemble simulations.

κ	β	ρ_{vap}	ρ_{liq}
3.9	1.85	0.16 ± 0.04	0.59 ± 0.03
	1.90	0.14 ± 0.05	0.61 ± 0.04
	1.95	0.11 ± 0.02	0.72 ± 0.02
	2.00	0.07 ± 0.02	0.74 ± 0.02
	2.05	0.07 ± 0.02	0.74 ± 0.02
7	2.50	0.32 ± 0.04	0.69 ± 0.05
	2.60	0.16 ± 0.02	0.84 ± 0.02
	2.70	0.13 ± 0.02	0.88 ± 0.02

change of mass with the solid phase will not occur. For this reason, points on the solid–liquid coexistence curve are usually located starting from explicit calculations of the free energy of both phases.[13] However, once we know a single set of points on the coexistence curve, no additional free energy calculations are needed to determine the remainder of that curve. Rather we can straightforwardly integrate the Clausius–Clapeyron equation,

$$\left(\frac{dP}{d\beta}\right)_c = -\frac{\Delta h}{\beta\Delta v} , \qquad (2)$$

where $\beta = 1/k_B T$, with k_B is the Boltzmann constant and T is the absolute temperature. P is the pressure, and $\Delta h = h_{II} - h_I$ and $\Delta v = v_{II} - v_I$ are the differences in molar enthalpy and molar volume in phase I and II, respectively. The subscript c denotes that the derivative is taken along the coexistence line. This is the approach that we followed in our work. The method that we used was based on a scheme due to Kofke.[14,15] We performed simulations for $\kappa = 3.9$, $\kappa = 7$, and $\kappa = 9$. The somewhat curious value $\kappa = 3.9$ was selected because for this value of κ, the Boyle temperature of the hard-core attractive Yukawa model equals that of the Girifalco model potential for C_{60} (Ref. 16) used in Ref. 9, if the well depth of the two potentials is chosen as the unit of energy and the point where the potential crosses zero is chosen as the unit of length. In Ref. 9 it was shown that the critical point for C_{60} is very close to the sublimation line. Hence, we could expect something similar for the Yukawa model with $\kappa = 3.9$. As will be shown below, the results for this Yukawa model are analogous, but certainly not identical, to the ones obtained for C_{60}.

The Gibbs ensemble simulations were performed for $\kappa = 3.9$ and $\kappa = 7$. As the liquid–vapor coexistence curve has already moved well into the metastable regime for $\kappa = 7$, we did not perform Gibbs-ensemble simulations for $\kappa = 9$. The Gibbs ensemble simulations were started with the density in each box initially equal to the estimated critical density, and

at a temperature that is equal to the critical temperature estimated by perturbation theory (see below). As first-order perturbation theory ignores fluctuations, we expect the actual critical temperature to be lower than this estimate and, indeed, we always found that at the initial temperature, the system was still in the one-phase region. Subsequently, we lowered the temperature in small steps until phase separation was observed. To check that the liquid and vapor phases had reached equilibrium, we verified that the chemical potentials of the systems in the "liquid" and "vapor" box were equal.

The Gibbs-ensemble simulations consisted of at least 30 000 cycles (i.e., trial moves per particle), denoted by N_{run}. One Gibbs-ensemble cycle consisted, on average, of one trial displacement of every particle, $N_{ex} = 50$ attempts to exchange particles between the two simulation boxes and $N_{vol} = 1$ attempt to exchange volume between the two boxes. All our simulations were performed for a system consisting of $N = 216$ particles. We chose such a relatively small system size to keep the computational cost within bounds, as many individual runs are needed to map out the phase diagram. The potential in these simulations was truncated and shifted at $r_c = 2$. The error introduced by this truncation is very small, even for $\kappa = 3.9$. In Table I we have collected the computed densities of the coexisting liquid and vapor phases for $\kappa = 3.9$ and $\kappa = 7$ as a function of temperature.

From these data the critical points could be estimated by using the law of rectilinear diameter[11] and assuming that the shape of the binodal is best described by a power law with the 3D-Ising exponent $\beta = 0.326$ (see Ref. 12). For $\kappa = 3.9$ the reciprocal critical temperature is estimated to be $\beta_c = 1.82 \pm 0.01$, and the critical density is $\rho_c = 0.37 \pm 0.02$. For $\kappa = 7$ the estimate of the reciprocal critical temperature is $\beta_c = 2.43 \pm 0.01$, with a critical density $\rho_c = 0.50 \pm 0.02$.

For our implementation of the Kofke integration scheme to trace out the melting curve, it is more convenient to write the Clausius–Clapeyron equation as

$$\left(\frac{d \ln \beta P}{d\beta}\right)_c = -\frac{\Delta e}{\beta P \Delta v} , \qquad (3)$$

where $\Delta e = e_{II} - e_I$ is the difference in molar energy between the two phases. The Kofke method can only be used to compute the phase coexistence curve, provided that one set of points on this curve is already known. In the present case, the

TABLE II. Settings during Gibbs–Duhem simulations. κ determines the range of the potential, $\Delta\beta$ is the step in reciprocal temperature, β_{init} is the initial reciprocal temperature, and β_{end} is the final reciprocal temperature.

κ	$\Delta\beta$	β_{init}	β_{end}
3.9	0.05	0.00	1.95
7	0.05	0.00	2.20
	0.01	2.00	2.28
9	0.05	0.00	2.35
	0.01	2.00	2.50

known point is the infinite temperature limit ($\beta\rightarrow0$), where the hard-core attractive Yukawa system reduces to the hard-sphere model. The pressure and densities of the coexisting phases of the hard-sphere model at melting are given by[17]

$$\rho_{fluid} = 0.943,$$

$$\rho_{solid} = 1.041, \qquad\qquad (4)$$

$$\beta P = 11.69.$$

In the high-temperature hard-sphere limit, the derivative in Eq. (3) is well-behaved and goes to a finite limit. Equation (3) was solved using a fourth-order predictor–corrector algorithm. As such algorithms are not self-starting, we initialized the integration using a first order predictor–corrector algorithm. After two time steps, a second order predictor–corrector algorithm was applied. After that, we continued with an integration routine of the desired order (4).

Clausius–Clapeyron integrations were used to determine the liquid–solid coexistence curves for $\kappa=3.9$, 7, and 9. In the simulations, the solid and the liquid phase are simulated simultaneously at the same temperature and pressure. By changing the pressure and temperature according to Eq. (3), we ensure the chemical potentials of the two phases also remain the same.

Table II shows the values of the various parameters that we used in the Clausius–Clapeyron integration. In our simulations, the maximum trial displacement of a particle was adjusted such that the acceptance of trial moves varied between 20% and 50%. Similar acceptance probabilities were maintained for the volume-changing moves. All simulations along the solid–fluid coexistence curve consisted of 10 000 equilibration cycles (N_{eq}) and 10 000 "production" cycles (N_{run}). We assumed that, in all cases, the structure of the solid phase was face-centered cubic. It is obvious that this structure (or the closely related hexagonal close-packed structure) must be the stable structure of the high-pressure or low-temperature solid. It seems plausible that the same structure is still thermodynamically stable at the melting point, although we have not tested this.

III. RESULTS

Combining the data obtained using the Gibbs-ensemble simulations and the Kofke integration scheme for $\kappa=3.9$, 7, 9, we obtain the phase diagrams shown in Fig. 2, 3, and 4.

As can be seen from the figures, the critical point for $\kappa=3.9$ is still well above the triple point temperature. However, for $\kappa=7$, the critical point has already crossed the sub-
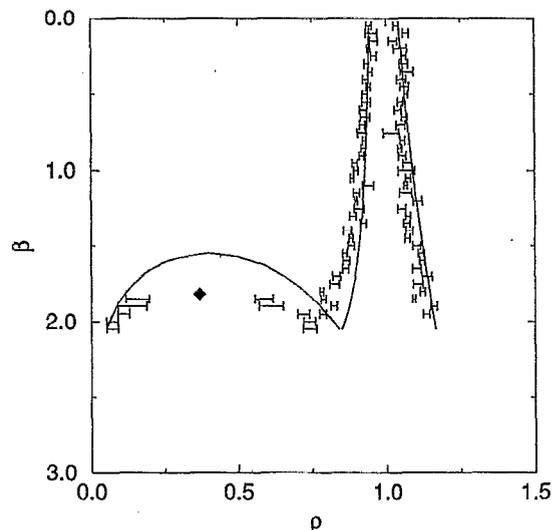

FIG. 2. Phase diagram for $\kappa=3.9$. In this figure the drawn lines correspond to the results of perturbation theory. The points with error-bars are the simulation results. The diamond indicates the critical point as obtained by Gibbs-ensemble simulations.

limation line. This implies that for $\kappa=7$ and, a fortiori, for $\kappa=9$, no stable liquid phase can exist. If we assume that the shift of the critical temperature relative to the sublimation curve is, to a first approximation, linear in κ, then no stable liquid phase is possible for attractive Yukawa systems with κ larger than approximately 6. It is interesting to note that, whereas for the κ values 7 and 9, the solid fluid coexistence curve could be integrated all the way down to temperatures where the solid coexists with dilute vapor, this was not possible for $\kappa=3.9$. The reason is that, for that value of κ, the sublimation line crosses the liquid–vapor binodal and spin-
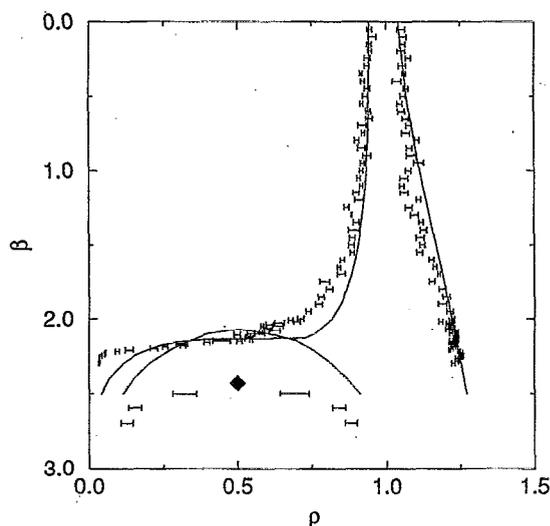

FIG. 3. Phase diagram for $\kappa=7$. In this figure the drawn lines correspond to the results of perturbation theory. The points with error-bars are the simulation results. The diamond indicates the metastable critical point as obtained by Gibbs-ensemble simulations.
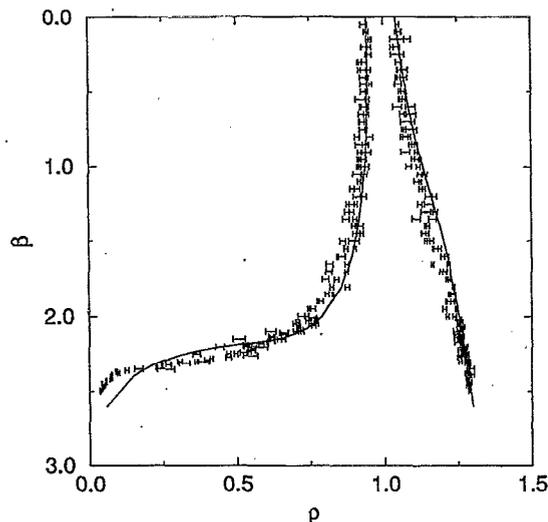
FIG. 4. Phase diagram for $\kappa=9$. The drawn lines correspond to the results of perturbation theory. The points with error-bars are the simulation results.

FIG. 5. Perturbation potential. The curves on the left denote the liquid phase, whereas the ones on the right denote the solid phase.

odal. In an infinite system, this would result in gas–liquid phase separation. However, in a finite periodic system the system remains homogeneous, but the pressure exhibits a van der Waals loop and the pressure may even go negative. When this happens, the integration of Eq. (3) breaks down. The fact that we observe this crossing of the spinodal only with $\kappa=3.9$ supports the conclusion that, only for this value of κ, the liquid–vapor coexistence curve crosses the sublimation line.

For the sake of comparison, we have also estimated the phase diagram of the attractive Yukawa system by simple first-order thermodynamic perturbation theory.[18] As a reference system, we use the hard-sphere fluid (solid). The excess Helmholtz free energy of the Yukawa system is estimated as

$$\beta F^{\text{ex}}(\rho) = \beta F^{\text{ex}}_{\text{HS}}(\rho) + \beta \langle U_P \rangle_{\text{HS}}, \qquad (5)$$

where the identification of $F^{\text{ex}}_{\text{HS}}$ is the excess free energy of the hard-sphere system at density ρ, and $\langle U_P \rangle_{\text{HS}}$ is the average value of the attractive part of the Yukawa potential, computed in the hard-sphere reference system. From Eq. (5), it is possible to derive all thermodynamic properties of the system needed to construct the phase diagram.

Simulations on a 108-particle hard-sphere fluid and hard-sphere (fcc) crystal were used to compute $\langle U_P \rangle_{\text{HS}}$. All simulations of the hard-sphere reference system consisted of 10 000 equilibration cycles and 10 000 "production" cycles. A plot of $\langle U_P \rangle_{\text{HS}}$ vs density ρ is shown in Fig. 5 for the relevant values of κ. We used the Carnahan–Starling equation to estimate the excess Helmholtz free energy of the hard-sphere fluid,[19] while the data of Hoover[17,20] were used to estimate the density-dependence of the free energy of the solid.

The estimated phase diagrams for $\kappa=3.9$, 5, 7, 9 are shown in Fig. 6. By construction, the liquid–vapor coexistence curve obtained by perturbation theory is characterized by a "classical" critical exponent ($\beta=1/2$). From Fig. 6 and
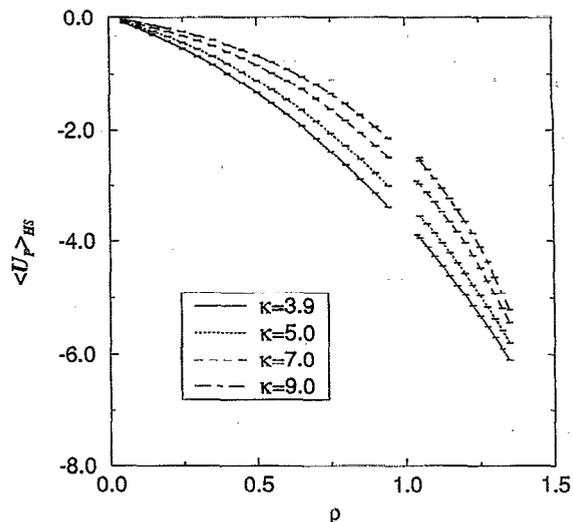
Table III it can be seen that perturbation theory predicts that there is no stable liquid phase when κ is larger than approximately 7.4 (this estimate was obtained by linear interpolation). We recall that the simulations of the hard-core Yukawa model indicate that the stable liquid already disappears around $\kappa \approx 6$. For the sake of comparison, we have drawn in Figs. 2–4 the phase-coexistence curves, as obtained by perturbation theory, as solid curves. From these figures it is clear that perturbation theory works reasonably well, in particular for the shorter-ranged potentials. However, perturbation theory systematically overestimates the critical temperature and, as a consequence, the value of κ for which the liquid phase disappears is overestimated by perturbation theory.
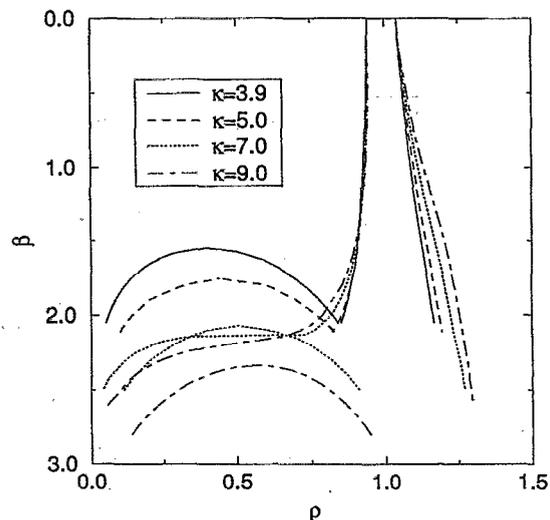

FIG. 6. Phase diagram of Yukawa system by first order perturbation theory.

TABLE III. Critical density p_c, critical reciprocal temperature β_c, and reciprocal triple temperature β_t as a function of κ as obtained from first order perturbation theory.

κ	p_c	β_c	β_t
3.9	0.40	1.55	2.07
5	0.44	1.75	2.10
7	0.50	2.07	2.13
9	0.57	2.34	

ACKNOWLEDGMENTS

[1] A. P. Gast, C. K. Hall, and W. B. Russel, J. Colloid Interface Sci. 96, 251 (1983).
[2] S. Asakura and F. Oosawa, J. Chem. Phys. 22, 1255 (1954).
[3] A. Vrij, Pure Appl. Chem. 48, 471 (1976).
[4] H. N. W. Lekkerkerker, W. C.-K. Poon, P. N. Pusey, A. Stroobants, and P. B. Warren, Europhys. Lett. 20, 559 (1992).
[5] P. N. Pusey, W. C. K. Poon, S. M. Ilett, and P. Barlett, J. Phys. 6, A29 (1994).
[6] F. Leal Calderon, J. Bibette, and J. Biais, Europhys. Lett. 23, 653 (1993).
[7] E. J. Meijer and D. Frenkel, Phys. Rev. Lett. 67, 1110 (1991).
[8] J. P. Hansen and L. Verlet, Phys. Rev. 184, 151 (1969).
[9] M. H. J. Hagen, E. J. Meijer, G. C. A. M. Mooij, D. Frenkel, and H. N. W. Lekkerkerker, Nature 365, 425 (1993).
[10] A. Z. Panagiotopoulos, Mol. Phys. 61, 813 (1987).
[11] J. S. Rowlinson and F. Swinton, Liquids and Liquid Mixtures (Butterworths Scientific, London, 1982).
[12] B. Smit, Ph. de Smedt, and D. Frenkel, Mol. Phys. 68, 931 (1989).
[13] NATO ASI on Computer Simulation in Materials Science, edited by M. Meyer and V. Pontikis (Kluwer Academic, Dordrecht, 1991).
[14] D. A. Kofke, J. Chem. Phys. 98, 4149 (1993).
[15] D. A. Kofke, Mol. Phys. 78, 1331 (1993).
[16] L. A. Girifalco, J. Phys. Chem. 96, 858 (1992).
[17] W. G. Hoover and F. H. Ree, J. Chem. Phys. 49, 3609 (1968).
[18] J. P. Hansen and I. R. McDonald, Theory of simple liquids (Academic, London, 1986).
[19] N. F. Carnahan and K. E. Starling, J. Chem. Phys. 51, 635 (1969).
[20] D. Frenkel and A. J. C. Ladd, J. Chem. Phys. 81, 3188 (1984).